LEVEL II

DNA 5738T

STRESS PULSE REFLECTION AND TENSILE CRACKING IN A ONE-DIMENSIONAL BILINEAR MATERIAL

R&D Associates
P.O. Box 9695
Marina del Rey, California 90291

31 December 1980

Topical Report for Period 1 November 1979—31 December 1980

CONTRACT No. DNA 001-80-C-0069

APPROVED FOR PUBLIC RELEASE;
DISTRIBUTION UNLIMITED.

THIS WORK SPONSORED BY THE DEFENSE NUCLEAR AGENCY
UNDER RDT&E RMSS CODE B310080464 P99QAXD800157 H2590D.

390124

Prepared for
Director
DEFENSE NUCLEAR AGENCY
Washington, D. C. 20305

Destroy this report when it is no longer needed. Do not return to sender.

PLEASE NOTIFY THE DEFENSE NUCLEAR AGENCY, ATTN: STTI, WASHINGTON, D.C. 20305, IF YOUR ADDRESS IS INCORRECT, IF YOU WISH TO BE DELETED FROM THE DISTRIBUTION LIST, OR IF THE ADDRESSEE IS NO LONGER EMPLOYED BY YOUR ORGANIZATION.

62704H

UNCLASSIFIED

SECURITY CLASSIFICATION OF THIS PAGE *(When Data Entered)*

REPORT DOCUMENTATION PAGE	READ INSTRUCTIONS BEFORE COMPLETING FORM
1. REPORT NUMBER: DNA 5738T	2. GOVT ACCESSION NO.: AD-A108833
3. RECIPIENT'S CATALOG NUMBER:	
4. TITLE *(and Subtitle)*: STRESS PULSE REFLECTION AND TENSILE CRACKING IN A ONE-DIMENSIONAL BILINEAR MATERIAL	5. TYPE OF REPORT & PERIOD COVERED: Topical Report for Period 1 Nov 79—31 Dec 80
	6. PERFORMING ORG. REPORT NUMBER: RDA-TR-113206-005
7. AUTHOR(s): D. A. Simons	8. CONTRACT OR GRANT NUMBER(s): DNA 001-80-C-0069
9. PERFORMING ORGANIZATION NAME AND ADDRESS: R & D Associates, P.O. Box 9695, Marina del Rey, California 90291	10. PROGRAM ELEMENT, PROJECT, TASK AREA & WORK UNIT NUMBERS: Subtask P99QAXDB001-57
11. CONTROLLING OFFICE NAME AND ADDRESS: Director, Defense Nuclear Agency, Washington, D.C. 20305	12. REPORT DATE: 31 December 1980
	13. NUMBER OF PAGES: 40
14. MONITORING AGENCY NAME & ADDRESS *(if different from Controlling Office)*	15. SECURITY CLASS *(of this report)*: UNCLASSIFIED
	15a. DECLASSIFICATION/DOWNGRADING SCHEDULE: N/A

16. DISTRIBUTION STATEMENT *(of this Report)*

Approved for public release; distribution unlimited.

17. DISTRIBUTION STATEMENT *(of the abstract entered in Block 20, if different from Report)*

18. SUPPLEMENTARY NOTES

This work sponsored by the Defense Nuclear Agency under RDT&E RMSS Code B310080464 P99QAXDB00157 H2590D.

19. KEY WORDS *(Continue on reverse side if necessary and identify by block number)*

Bilinear materials
Tensile cracking materials
Stress waves
Spall

20. ABSTRACT *(Continue on reverse side if necessary and identify by block number)*

As a check case for numerical studies of tensile cracking in nonlinear media, closed form solutions have been derived for the following problems. A finite slab of bilinear material is loaded on one face by a sharp-fronted triangular pressure pulse. Cracks are assumed to form in the first case when the stress exceeds a tensile limit for a finite time, i.e., the tensile impulse is finite. In both cases the stress reaches the tensile limit and a first crack forms shortly after the incident wavefront reflects from the

DD FORM 1 JAN 73 1473 EDITION OF 1 NOV 65 IS OBSOLETE

UNCLASSIFIED

SECURITY CLASSIFICATION OF THIS PAGE *(When Data Entered)*

20. ABSTRACT (Continued)
free face of the slab. In the first case a continuously cracked zone develops under the action of a tensile spike caused by the first crack. In the second case, the tensile spike has no effect on cracking, and a sequence of discrete cracks form. Stress histories and stress profiles are plotted for both cases.

TABLE OF CONTENTS

LIST OF ILLUSTRATIONS

I. INTRODUCTION

In finite-difference calculations of transient ground motion, it has proven useful to incorporate artificial viscosity as a means of smoothing out shocks and reducing the numerical noise they generate. Noise may also be generated by the transition between loading and unloading in a hysteretic solid, or by the appearance of a tensile crack in a material element, should the constitutive law include some criterion for the formation of cracks normal to the direction of the stress. In the numerical analysis of such materials, there is a possibility that noise generated by shocks, stress reversals, or cracks could cause subsequent spurious cracking and serious deviation from the correct response. Artificial viscosity may alleviate this problem, but must be used with caution so it does not cause deviations from the correct response.

In this report an exact analytic solution is derived for the propagation and reflection of a particular stress pulse in a hysteretic, tensile-cracking material. Stress histories and crack locations are presented in a form convenient for comparison with numerical code output. The solution thus may be used as a check on code calculations and as a tool for the selection of the optimum artificial viscosity.

The problem solved is for a material with no viscosity and consequently no shock smoothing. However, in order to clarify certain features of the solution, it will prove useful to regard it in a sense as the limit of a sequence of solutions for materials with smaller and smaller viscosities.

Two different possible versions of the tensile cracking model will be included. In the first one, cracks form whenever the stress exceeds a tensile cutoff, regardless of the duration of the tensile pulse. In the second, the tensile

cutoff stress must be reached and in addition must persist for a finite (but very short) time, i.e., the tensile impulse must not vanish. As applied to the present solution, these models differ only in that a tensile spike can cause a crack in the first instance but has no effect on cracking in the second. However, this distinction will be seen to cause a marked difference in the resulting crack patterns.

The loading analyzed is a sharp-fronted triangular pressure pulse applied to one face (the loaded face) of a free slab of bilinear material. During the initial propagation of the pulse through the slab toward the other face (the free face), it remains compressive but its shape changes due to the hysteresis in the stress-strain law. After reflection the stress between the free face and the reflected wave front becomes tensile, with the maximum tensile stress (at the wave front) increasing with time. When this maximum reaches the tensile cutoff stress, a crack will form at the wave front regardless of which cracking criterion is used, and a finite spall layer will separate from the rest of the slab.

What happens next depends on which cracking model is employed. For the simple tensile cutoff criterion, a continuously cracked region develops in the main part of the slab behind the reflected wave front as it continues to propagate back toward the loaded face. In the example to be worked out, continuous cracking proceeds all the way back to the loaded face, leaving only the originally spalled layer intact.

If a finite but very small tensile impulse is required for cracking, then after the first crack forms, a discrete set of cracks appears. The reason is that the formation of the first crack leaves a tensile spike at the reflected

wave front. As mentioned above, the spike can contribute to cracking in the simple tensile cutoff model but has no effect in the finite impulse model. In the numerical example to be presented, three discrete cracks form, leaving a slab between the last crack and the loaded face containing a stress spike that reflects back and forth.

Some of the events just described are clearly beyond the capability of any numerical code to predict exactly. As is well known, the closest (and most useful) possible numerical representation of a sharp-fronted pulse is one with the front smeared--by artificial viscosity--over several zones. The continuously cracked region could at best be modeled as a sequence of adjacent zones, each with a tensile crack. The best approximation of a spike would be a pulse several zones wide. The problem thus provides a severe test for any code, but not an unreasonable one, because the ground motion problems of greatest interest contain at least some of these difficult features.

II. TENSILE CRACKING IN AN ELASTIC MATERIAL

Before solving the problems posed for bilinear media, it will be useful to discuss several related problems in elastic media. The need for this discussion stems from the fact that in bilinear media only sharp-fronted pulses can be analyzed in closed form, while in elastic media those with finite rise times can be treated exactly by the method of images. Finite rise times are of interest because the cracking process caused by a sharp-fronted pulse will be regarded as the limit of a sequence of processes caused by pulses with finite but shorter and shorter rise times. Because one effect of viscosity is to smooth out shocks, letting the rise time tend to zero models in a crude way the effect of letting viscosity tend to zero. (The correspondence is not exact because the triangular pulse shapes to be considered will not be rounded off as those in a viscous solid would be. However, it may be argued that the limit is the same.)

Consider then the reflection of the triangular stress pulse shown in Figure 1a. It impinges from the left on a free surface located at the vertical axis. Compressive stresses are plotted upward. The stresses at three successive instants of time are shown as the solid lines labeled 1, 2, and 3. These are obtained by superposing the rightward propagating incident pulse with its negative images propagating to the left. At instant 3 the stress has reached the tensile cutoff and a crack forms at that location, labeled C. The crack will form regardless of whether the simple tensile cutoff criterion or the small but finite tensile impulse criterion is invoked, although in the latter case it would form slightly later. The picture at instant 3 is repeated in Figure 1b, but the spalled material to the right of the crack has been removed to emphasize that at later times the left-hand side of the crack acts as a new reflecting surface.

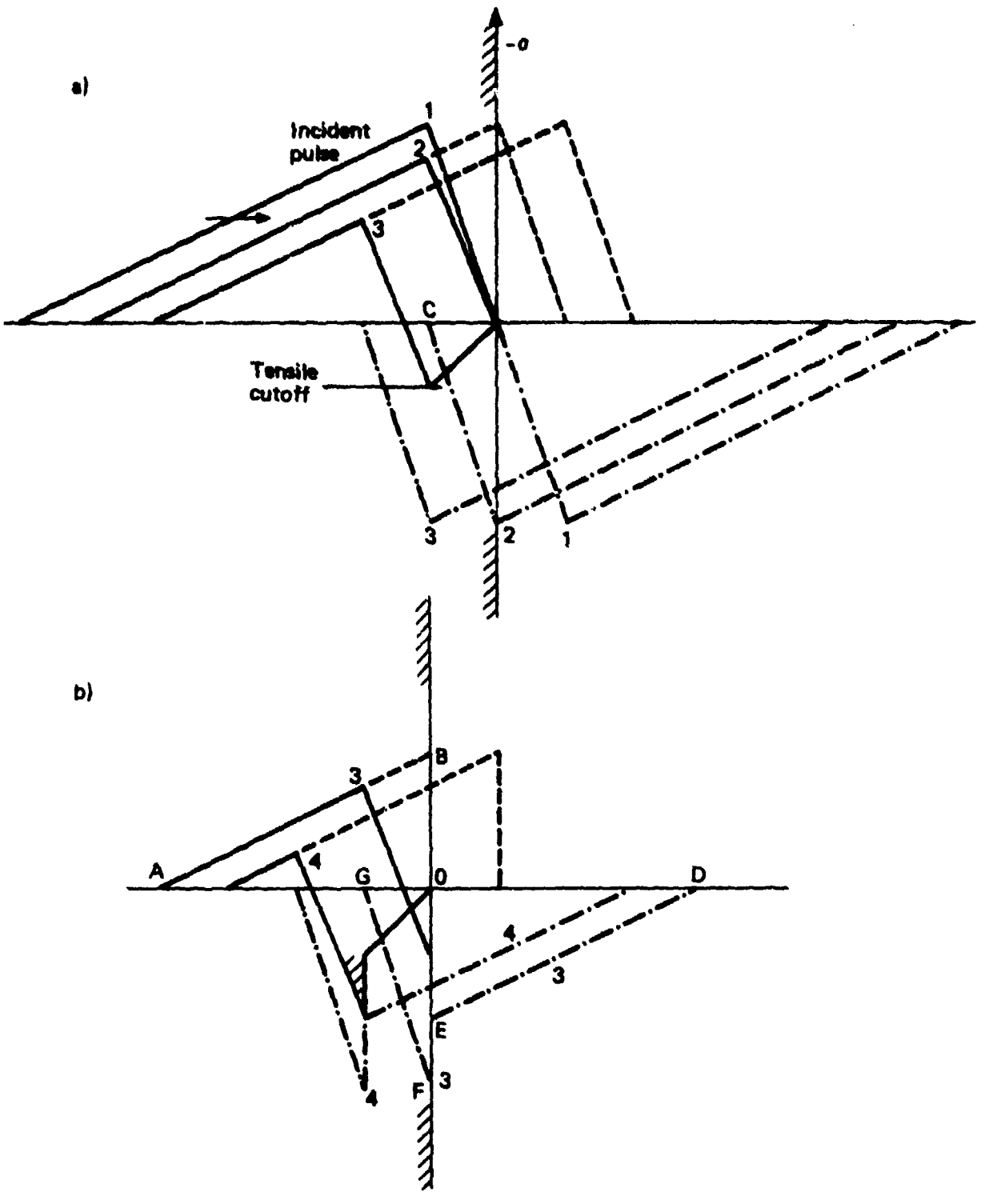

Figure 1. Reflection of a pulse with finite rise time in an elastic material (a) before cracking, (b) hypothetical situation after first crack, assuming no second crack.

To see what happens next, suppose for the moment that no new cracks will form. The stress at later times would then be the superposition of three triangular pulses:

1. The part of the incident wave that was not removed with the spall layer, propagating to the right (OAB),
2. The negative image of OAB, propagating to the left (ODE), and
3. The part of the original negative image pulse that was not removed with the spall layer, propagating to the left (OFG).

As represented by the shading in Figure 1b, at the later time 4 the wave would contain a narrow triangular tensile pulse of height equal to the tensile cutoff stress propagating to the left. If the simple tensile cracking criterion had been maintained, this pulse would have caused a second crack to form immediately after the first one. In fact, a continuously cracked region would form. On the other hand, if the finite impulse criterion had been in force, this narrow pulse might or might not cause cracking, depending on its width. If it were not wide enough, then a second crack would not form until later, and it would be a finite distance from the first.

Figure 2 shows the same sequence for an incident pulse with a shorter rise time. By comparison, we see that the first crack forms at the same place and that the narrow tensile pulse has the same height but less width. Figure 3 shows the limit as rise time tends to zero. The narrow tensile pulse has become a spike with no impulse and could not contribute to cracking by the finite impulse criterion; however, it still could by the simple tensile cutoff criterion. Thus the solid curve labeled 4 would actually apply in the former case, and an instant later a second crack would form since the tensile impulse would become finite due to the broadened tensile pulse that follows. On the other hand, under the simple tensile

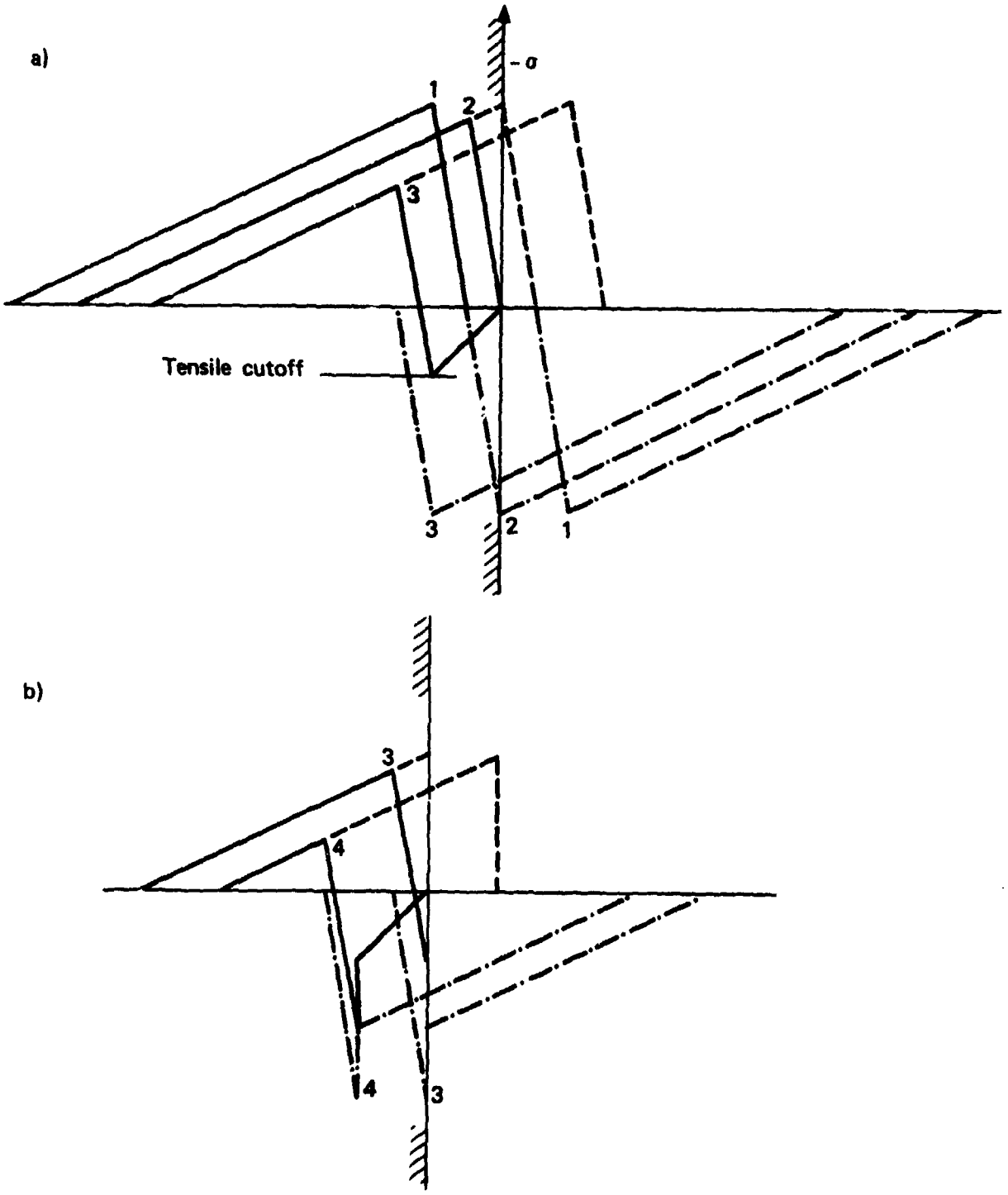

Figure 2. Reflection of a pulse with shorter rise time than in Figure 1.

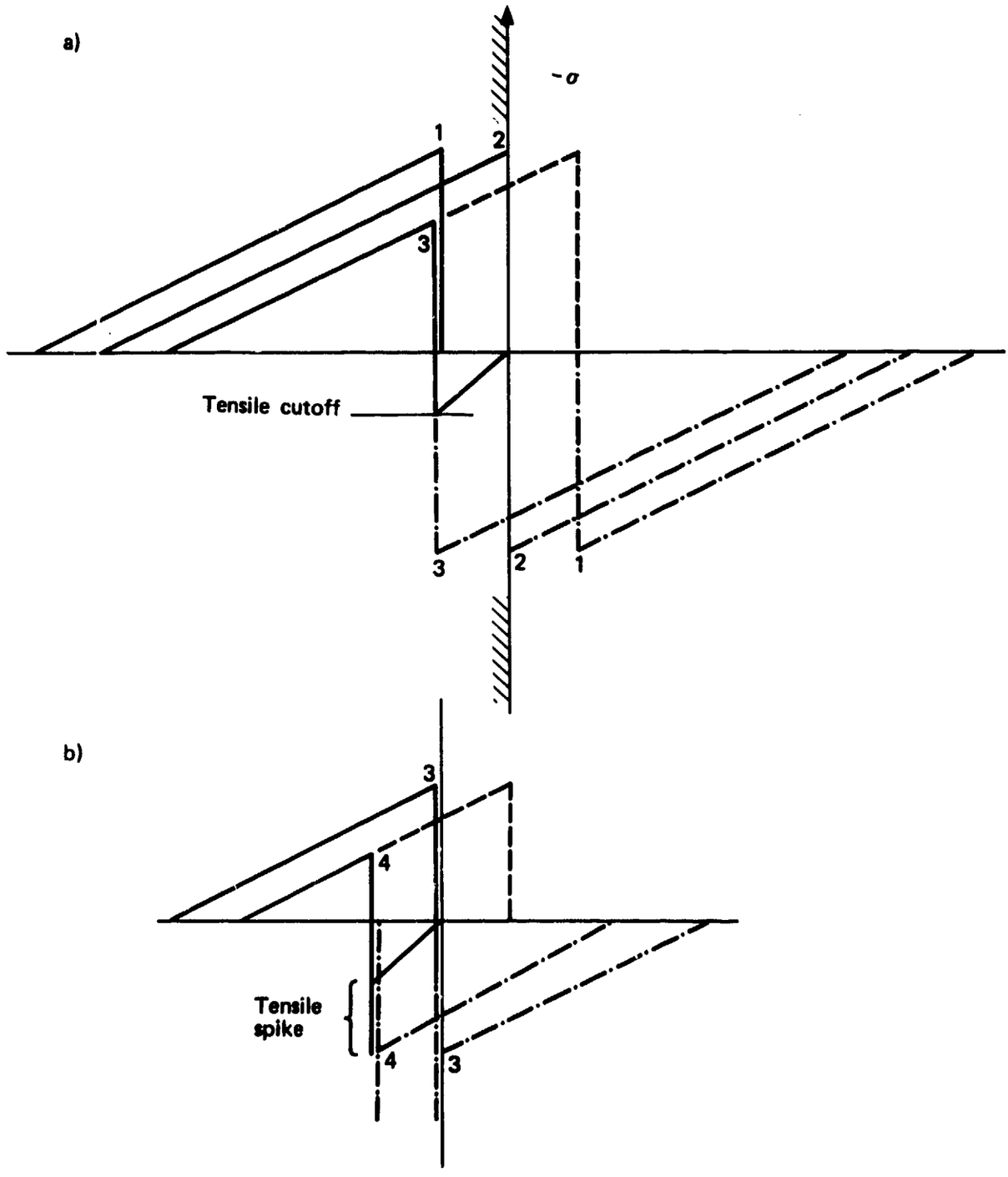

Figure 3. Reflection of a sharp-fronted pulse in an elastic material.

cutoff criterion curve 4 would never develop; rather the tensile spike would cause a continuous cracked zone to form between the first crack and the reflected wave front.

Figure 4a shows in more detail the development of the continuously cracked region under the simple tensile cutoff criterion for the incident pulse with finite rise time of Figure 2a. The picture at time 3 when the first crack has just formed has been repeated. At the later time 4, the cracking has progressed to a point determined by the superposition of the decaying tail of the incident pulse and the rising front of reflection of the original incident pulse. All parts of either pulse between the current crack location and the first crack become irrelevant; in particular, the image pulse ODE never influences the future cracking (it does, however, contribute to the stresses in the spalled layer between the first crack and the original free surface). In effect, the height of the rising front of the reflected pulse is progressively eroded until slightly after time 5 when it passes the end of the incident pulse. At later times such as 6, all that remains is a narrow triangular tensile pulse with height equal to the tensile cutoff propagating to the left.

Figure 4b shows the same sequence for the sharp-fronted incident pulse of Figure 3a, when the simple tensile cutoff criterion is used. Continuous cracking ceases at time 5, and at the typical later time 6 all that remains is a leftward propagating tensile spike equal to the tensile cutoff.

The foregoing discussion has shown how a tensile spike is formed after the first crack in a linear medium and how the spike influences subsequent cracking. Both the spike formation and its influence will be similar for a bilinear medium, and this will be analyzed in the next two sections.

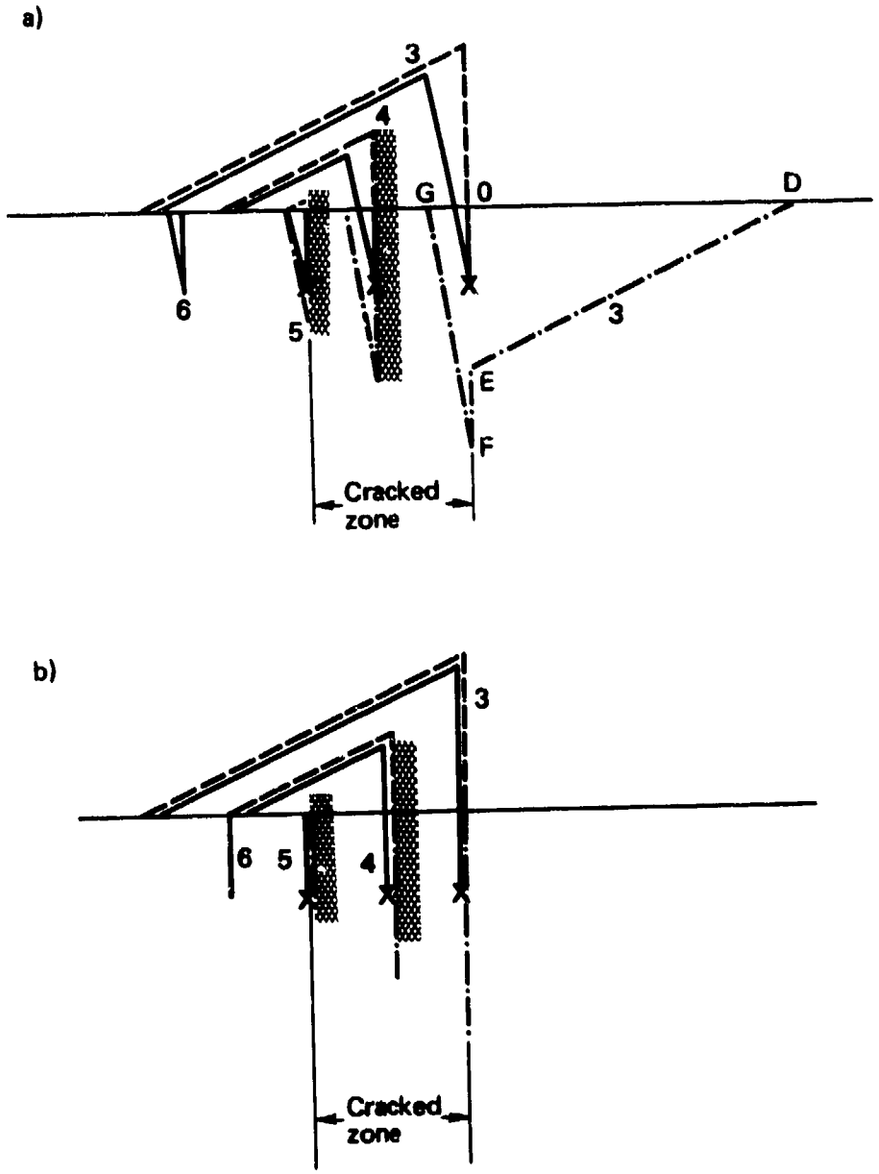

Figure 4. Development of the continuously cracked zone in an elastic solid with no tensile impulse requirement. (a) finite rise time, (b) sharp-fronted pulse.

III. FORMULATION OF THE PROBLEM FOR A BILINEAR MEDIUM

A slab of material occupies the region $0<x<\ell$, $-\infty<(y,z)<\infty$. The face $x=0$ is uniformly loaded by a sharp-fronted triangular pressure pulse

$$p(t) = -\sigma(0,t) = \begin{cases} 0, & t<0 \\ p_o(1-t/t_o), & 0<t<t_o \\ 0, & t>t_o \end{cases} \tag{1}$$

where $\sigma(x,t)$ is the stress (taken positive in tension), p_o is the peak applied pressure, and t_o the duration of the loading pulse. The material is a "bilinear" solid with stress-strain law

$$\sigma(x,t) = E_\ell \, \varepsilon(x,t) \tag{2a}$$

on initial loading, and

$$\sigma(x,t) = \sigma_m(x) - E_u[\varepsilon_m(x) - \varepsilon(x,t)] \tag{2b}$$

on unloading or reloading below the previous maximum compressive stress.* Here E_ℓ and $E_u>E_\ell$ are the loading and unloading moduli in plane strain, ε is the strain, and $\varepsilon_m(x)<0$ and $\sigma_m(x)=E_\ell\varepsilon_m(x)$ are the most compressive strain and stress attained at a given x. The material is assumed to have a tensile cutoff stress σ_{tco}. Both the simple tension and the finite tensile impulse criteria for cracking will be considered.

The equation of motion is

$$\frac{\partial \sigma}{\partial x} = \rho \frac{\partial^2 u}{\partial t^2} \tag{3}$$

*In the sequel, "reloading" will mean "reloading below the previous maximum compressive stress."

where ρ is the density and u the displacement in the x-direction. With the assumption of small displacements and strains, the density may be taken as constant, there is no distinction between Lagrangian and Eulerian coordinates, and the strain-displacement relation is

$$\varepsilon = \frac{\partial u}{\partial x} \ . \tag{4}$$

An ordinary wave equation with wave speed $c_\ell = (E_\ell/\rho)^{\frac{1}{2}}$ governs the displacement u during initial loading, as can be shown by combining Eqs. (2a), (3) and (4). For unloading or reloading, substituting Eq. (4) into Eq. (2b) and that result into Eq. (3) yields the inhomogeneous wave equation

$$\frac{\partial^2 u}{\partial x^2} - \frac{1}{c_u^{\,2}} \frac{\partial^2 u}{\partial t^2} = \left(\frac{1}{E_\ell} - \frac{1}{E_u}\right) \frac{d\sigma_m}{dx} \tag{5}$$

where $c_u = (E_u/\rho)^{\frac{1}{2}}$ is the unloading wave speed. The loading-unloading boundary (in the x-t plane) is in general impossible to locate analytically. However, for the sharp-fronted loading of Eq. (1), it is trivial: loading occurs only at the leading wave front before reflection, which propagates at speed $c_\ell < c_u$. In every finite disturbed region of the x-t plane, only unloading or reloading occurs, Eq. (5) applies, and c_u is the characteristic speed.

The general solution of Eq. (5) is

$$u(x,t) = f(t-x/c_u) + g(t+x/c_u) + \left(\frac{1}{E_\ell} - \frac{1}{E_u}\right)\int_o^x \sigma_m(\xi)\,d\xi \tag{6}$$

and from Eqs. (2) and (4) the corresponding stress is

$$\sigma(x,t) = -\frac{E_u}{c_u}\left[f'(t-x/c_u) - g'(t+x/c_u)\right] \ , \tag{7}$$

where primes denote differentiation with respect to the argument. The rest of the problem is to find expressions for the

as yet arbitrary functions f, g, and σ_m, and concurrently to determine when and where cracking occurs.

IV. SOLUTION

The x-t plane (or characteristic plane) is shown in Figure 5 for a slab of thickness 2.5 $c_\ell t_o$ and for $c_u/c_\ell = 2$. Line OBC is the loading front propagating at speed c_ℓ. Below this line the material is at rest and above it the material is unloading or reloading, so Eqs. (6) and (7) apply. The plane is subdivided by certain critical characteristics $t \pm x/c_u$ = const., and the functional form of the solution will be different in each region.

We begin with region OAB, bounded by the loading wave front, the loaded portion of the time-axis, and the wave front moving to the right at speed c_u from the tail of the loading pulse. Here the following conditions must hold:

1. The stress at the loaded end must equal the negative of the applied pressure,

$$\sigma(0,t) = -p(t) \ . \tag{8}$$

2. The stress along the leading wave front must be the maximum compressive stress,

$$\sigma(c_\ell t,t) = \sigma_m(c_\ell t) \ . \tag{9}$$

3. The displacement along the leading wavefront must vanish,

$$u(c_\ell t,t) = 0 \ . \tag{10}$$

By substituting Eqs. (6) and (7) for u and σ into Eqs. (8-10), differentiating (10) with respect to t, and rearranging, we find

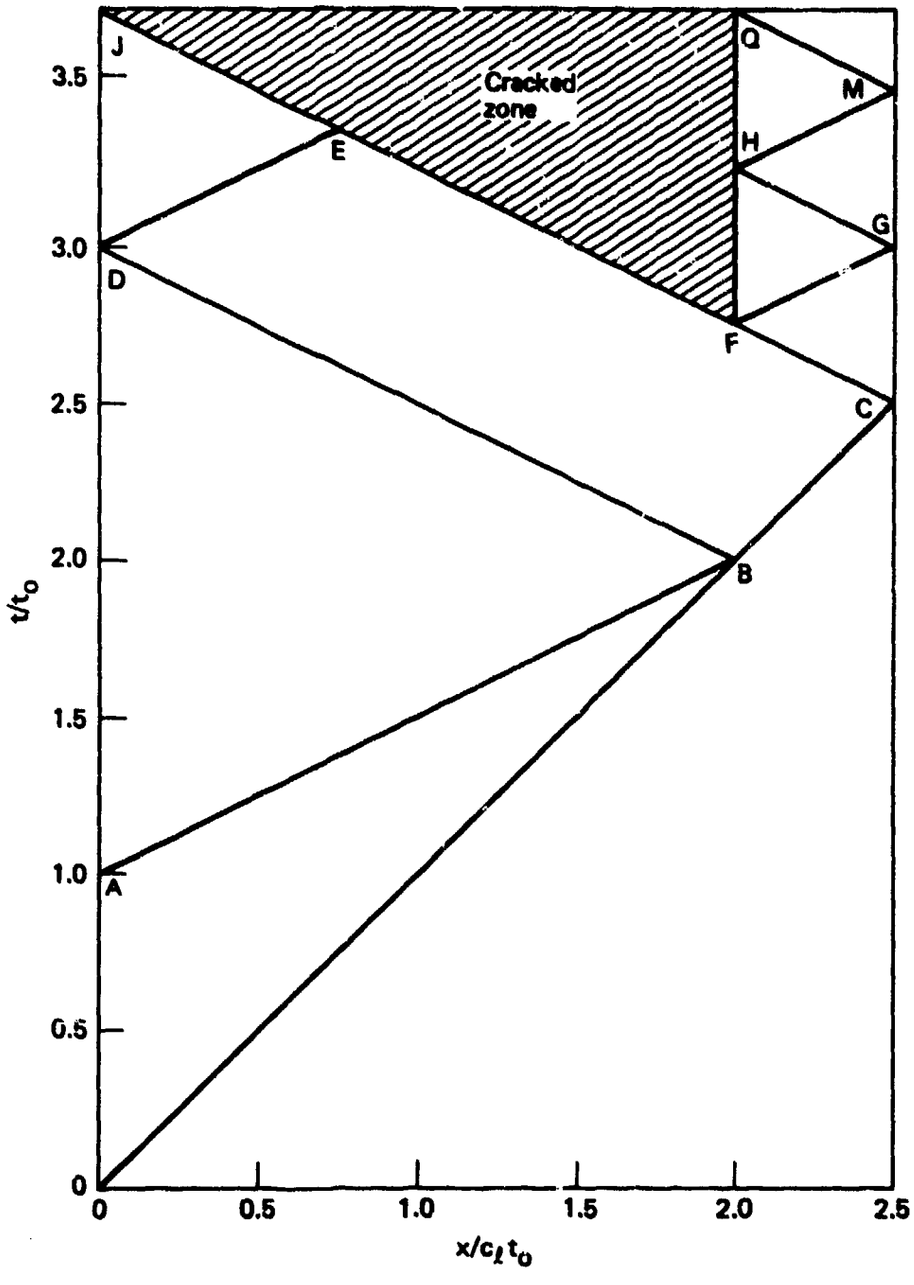

Figure 5. Characteristic plane for $\ell = 2.5\ c_\ell t_o$, $c_u/c_\ell = 2$, and for cracking by the simple tensile cutoff criterion.

$$\left.\begin{aligned} &f'[t(1-\gamma)] - g'[t(1+\gamma)] + h(t) = 0 \ , \\ &f'[t(1-\gamma)] + \frac{1+\gamma}{1-\gamma}\, g'[t(1+\gamma)] + \frac{1+\gamma}{\gamma}\ h(t) = 0 \ , \\ &f'(t) - g'(t) = s(t) \ , \end{aligned}\right\} \qquad (11)$$

where $\gamma = c_\ell/c_u$, $h(t) = c_u\sigma_m(c_\ell t)/E_u$, and $s(t) = c_u p(t)/E_u$. Since $s(t)$ is a linear function of t, viz.,

$$s(t) = \frac{c_u p_o}{E_u}\left(1 - \frac{t}{t_o}\right) ,$$

the above system of equations can easily be solved by assuming that each of the unknown functions f', g', and h is a linear function of its argument and equating coefficients of the constant and linear terms on each side of the equations. The results for region OAB are thus

$$\frac{E_u g'(t)}{c_u p_o} = \frac{1-\gamma}{2\gamma} - \frac{(1-\gamma)^2}{4\gamma}\,\frac{t}{t_o} \ , \qquad (12)$$

$$\frac{E_u f'(t)}{c_u p_o} = \frac{1+\gamma}{2\gamma} - \frac{(1+\gamma)^2}{4\gamma}\,\frac{t}{t_o} \ , \qquad (13)$$

$$-\frac{\sigma_m(x)}{p_o} = 1 - \frac{1-\gamma^2}{2}\,\frac{x}{c_\ell t_o} \ , \qquad (14)$$

and from Eq. (7),

$$-\frac{\sigma(x,t)}{p_o} = 1 - \frac{t}{t_o} + \frac{1+\gamma^2}{2}\,\frac{x}{c_\ell t_o} \ . \qquad (15)$$

Next consider region ABD. Because the backward characteristics $t+x/c_u$ = const. are common between this region and OAB, $g'(t)$ will still be given by Eq. (12). A new formula is needed for $f'(t)$, and it follows from the condition that $\sigma(0,t) = 0$. From Eqs. (7) and (12) this yields for region ABD,

$$\frac{E_u f'(t)}{c_u p_o} = \frac{1-\gamma}{2\gamma} - \frac{(1-\gamma)^2 t}{4\gamma t_o} \tag{16}$$

$$-\frac{\sigma(x,t)}{p_o} = \frac{(1-\gamma)^2 x}{2c_\ell t_o} \quad . \tag{17}$$

Note that the stress-free surface condition gave $f'(t) = g'(t)$. Considering that the stress is proportional to the difference of these functions [see Eq. (7)], the method of images could have been used to obtain $f'(t)$ and the stress, just as in the linear problem. The difference here is that the incident portion, which for this reflection is the backward propagating function $g'(t+x/c_u)$, could not have been found simply by tracing backwards to the initial loading as in the linear problem.

In region BCED, the function $f'(t)$ will still be given by Eq. (16) since the forward characteristics $t-x/c_u = \text{const.}$ are common between this region and ABD. Conditions (9) and (10) must still apply, and may be used in similar fashion to obtain for region BCED

$$\frac{E_u g'(t)}{c_u p_o} = \frac{(1-\gamma)^2}{2\gamma(1+\gamma)} \left[1 - \frac{(1-\gamma)^2 t}{2(1+\gamma)t_o}\right] , \tag{18}$$

$$\sigma(x,t) = -p_o \frac{1-\gamma}{1+\gamma} \left[1 - \frac{(1-\gamma)t}{(1+\gamma)t_o} + \frac{(1+\gamma^2)(1-\gamma)x}{2(1+\gamma)c_\ell t_o}\right] ,$$

$$-\frac{\sigma_m(x)}{p_o} = \frac{1-\gamma}{1+\gamma} \left[1 - \frac{(1-\gamma)^2 x}{2c_\ell t_o}\right] .$$

At this stage the maximum $\sigma_m(x)$ has been determined for the entire slab and only f' and g' need be calculated in the remaining regions. These can easily be found at each stage by imposing a stress-free boundary condition at either end or on both faces of any cracks that form, provided that the tensile spike caused by cracking is included properly.

The incident pulse first reflects from the free surface into region CFG of Figure 5. The function f' is the same as for the adjacent region BCED [see Eq. (16)], and g' follows as a simple reflection of f' according to the stress-free condition at $x = \ell = 2.5\, c_\ell t_o$ and Eq. (7):

$$\frac{E_u g'(t)}{c_u p_o} = \frac{1-\gamma}{2\gamma} - \frac{(1-\gamma)^2 (t-2\ell/c_u)}{4\gamma t_o}$$

$$-\frac{\sigma(x,t)}{p_o} = -\frac{(1-\gamma)^2 (\ell-x)}{2c\ell t_o} \qquad (19)$$

Note that just after this first reflection, the stress is tensile, independent of time, and linearly increasing with distance from the end, just as in the linear solid of Figure 3a.

The tensile cutoff stress σ_{tco} is taken to be $\sigma_{tco} = p_o/16$. With $\ell = 2.5\, c_\ell t_o$ and $\gamma = 1/2$, Eq. (19) shows that the first crack occurs at $x = 2c_\ell t_o$, and knowing the slopes of the characteristics in Figure 5 we find the time of cracking corresponding to point F to be $2.75\, t_o$.

Stress profiles are shown in Figure 6 up to this time. The vertical positions agree with the time scale of Figure 5 and the horizontal scales are the same so the plots may be overlain.

The subsequent behavior depends on whether a finite impulse is required for cracking. First we suppose it is not, so that the tensile spike just ahead of the first crack can cause continuous cracking. Cracking will begin at $x = 2c_\ell t_o$ and propagate to the left along FE in Figure 5 with speed c_u. The problem now is to determine when crack-cracking ceases. To do so, we proceed just as in the elastic analysis; i.e., we suppose that cracking has ceased and then check the stress at the next instant to see if the tensile

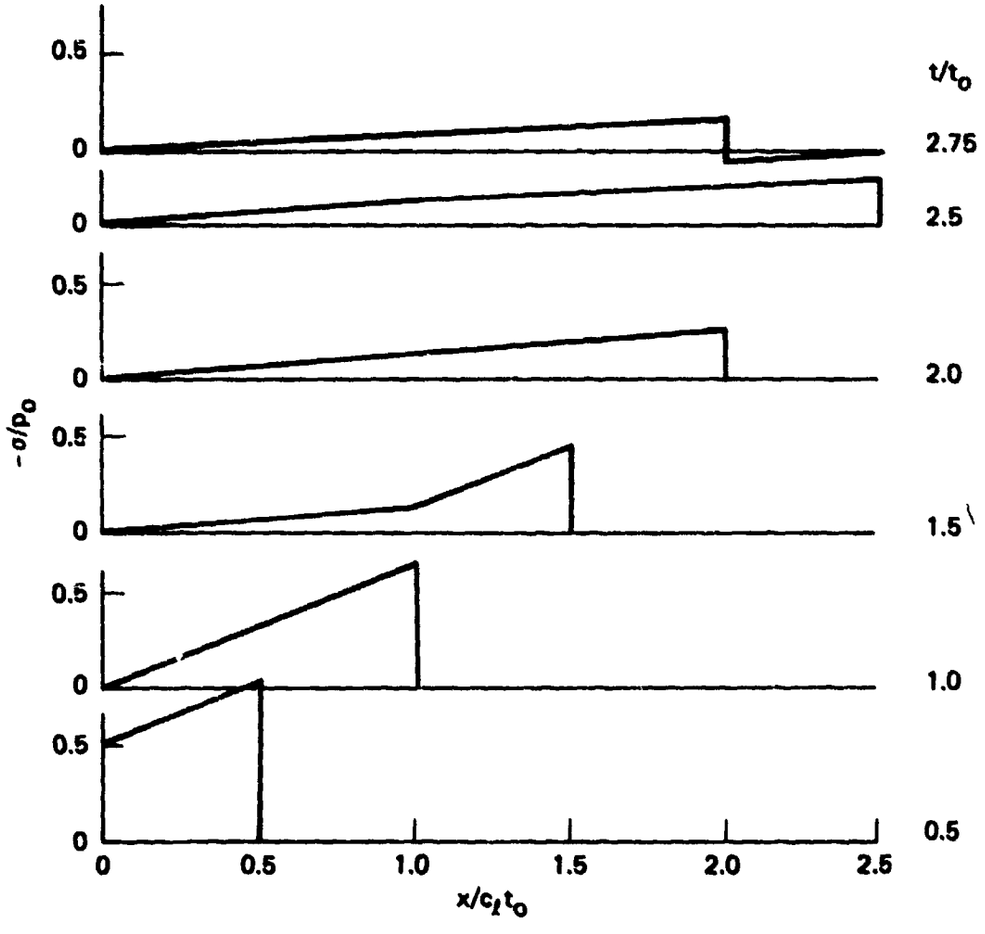

Figure 6. Stress profiles up to the time of initial cracking in a bilinear solid.

cutoff has been exceeded. In region BCED f' is given by Eq. (16), and if cracking were to cease somewhere along FE, then to the left of the crack Eq. (16) would continue to hold across the remaining part of EF. Since CE is given by $t + x/c_u = 3.75\ t_o$ we find from Eq. (16) that along CE

$$\frac{E_u f'(t-x/c_u)}{c_u p_o} = \frac{1-\gamma}{2\gamma} - \frac{(1-\gamma)^2(3.75t_o-2x/c_u)}{4\gamma t_o} \quad . \tag{20}$$

As long as cracking continues the value of the spike in g' on FE is simply that which, when combined with the f' above per Eq. (7) gives σ_{tco}. If cracking were to cease at some point along FE, then at the next instant on FE a bit to the left g' would be the same but f' in Eq. (20) would have decreased (since x decreased), so the stress per Eq. (7) would have become more tensile. But the tensile limit cannot be exceeded, so a contradiction is reached and we conclude that cracking must proceed at least as far as point E.

To see if cracking goes further, we must find a new f' for region DEJ. This follows from the reflection at x = 0 of g' for BCED as given by Eq. (18), and in fact f'(t) will be given by the same formula as g'(t) in Eq. (18). Thus on EJ

$$\frac{E_u f'(t-x/c_u)}{c_u p_o} = \frac{(1-\gamma)^2}{2\gamma(1+\gamma)}\left[1 - \frac{(1-\gamma)^2(3.75t_o-2x/c_u)}{2(1+\gamma)t_o}\right] .$$

Because this decreases when x decreases, the same reasoning as before leads to the conclusion that cracking must continue. Therefore the rest of the bar becomes continuously cracked, so that when the leading wave front has returned to the loaded face at $t = 3.75\ t_o$, the only part of the slab that remains intact is the original spalled layer from $x = 2c_\ell t_o$ to $2.5\ c_\ell t_o$.

The stresses in this part are periodic in time and can be obtained by reflections of f' from Eq. (16).

Stress profiles on an expanded stress scale are shown in Figure 7 for times after the first crack, and stress histories are shown in Figure 8 for several locations. The characteristic plane is redrawn in Figure 9 for reference from Figure 8.

We now turn to the finite impulse cracking criterion, in which case the tensile spike caused by the first crack will not have any effect on subsequent cracking. In the numerical example all the results below the characteristic CFEJ in Figure 5 are still valid, as are those in the initial spalled zone between $x = 2c_\ell t_o$ and $2.5\ c_\ell t_o$. The left-hand face of the first crack now may be treated as a new free surface. With reference to the characteristic plane as redrawn in Figure 10, in zone FHK f' will come from zone BCED [Eq. (16)], and g' will be the reflection of this at $x = 2c_\ell t_o$, giving

$$\frac{E_u g'(t)}{c_u p_o} = \frac{1-\gamma}{2\gamma}\left[1 - \frac{(1-\gamma)(t-2t_o)}{2t_o}\right]$$

$$-\frac{\sigma}{p_o} = \frac{(1-\gamma)^2}{2}\left[\frac{x}{c_\ell t_c} - 2\right]. \qquad (21)$$

Directly on FK g' will be a spike with value just sufficient to have caused the first crack. For the numerical values chosen this is given by $E_u g'_{FK}/c_u p_o = 11/32$. By comparison with the elastic case of Figure 2b, the proper interpretation is that this value continues to propagate along FK and beyond, even after subsequent cracks have appeared. The next crack forms when the stress given by Eq. (21) reaches σ_{tco}, and this will be at $x = 1.5\ c_\ell t_o$ and $t = 3t_o$.

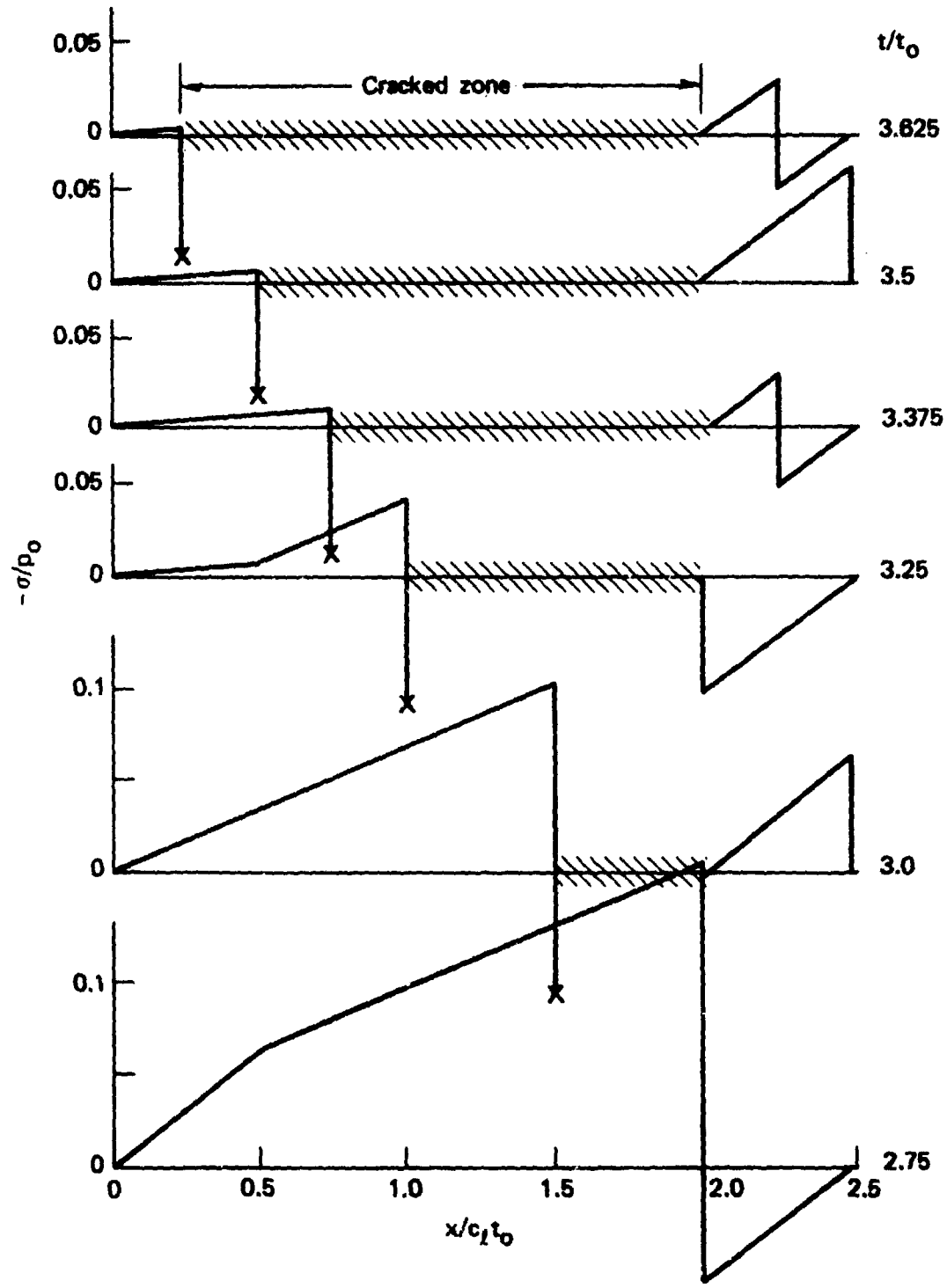

Figure 7. Stress profiles after initial cracking by the simple tensile cutoff criterion.

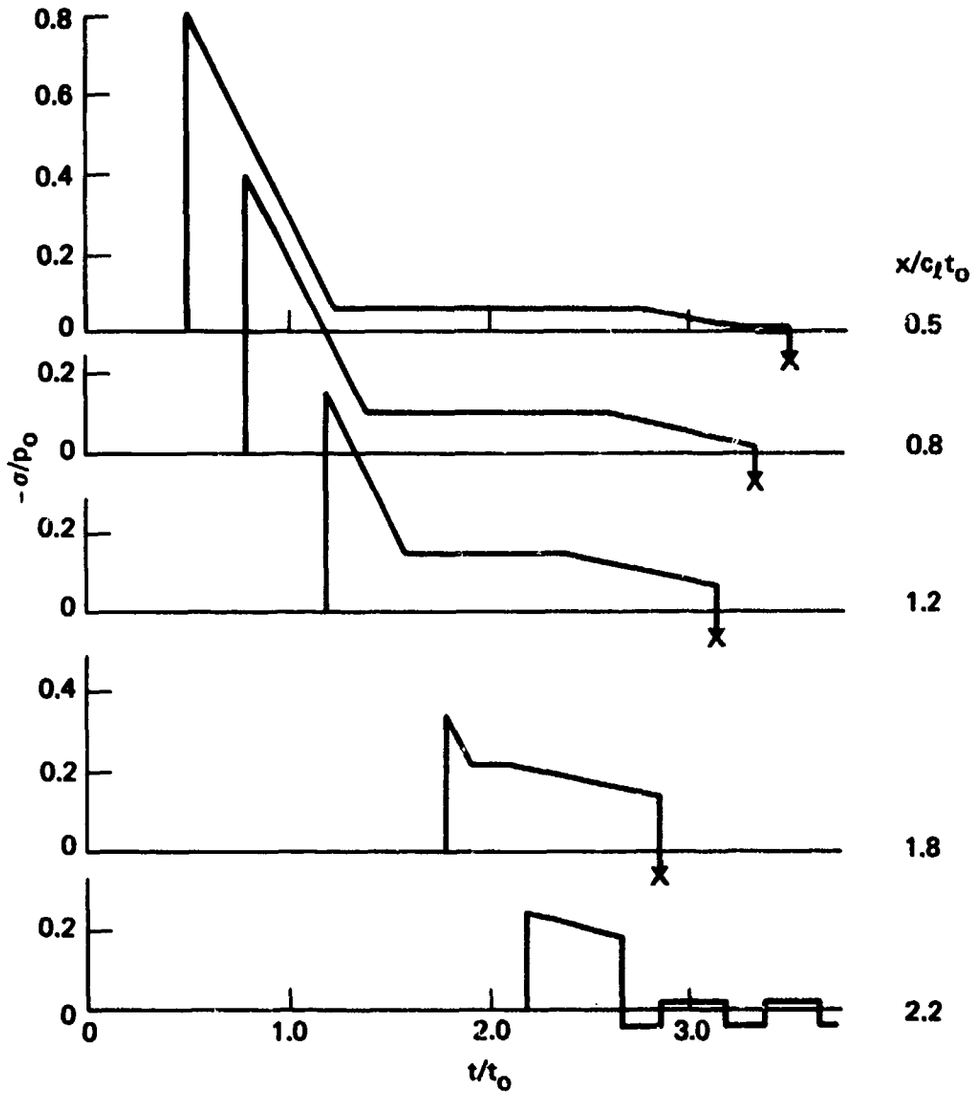

Figure 8. Stress histories in a bilinear solid with a simple tensile cutoff cracking criterion.

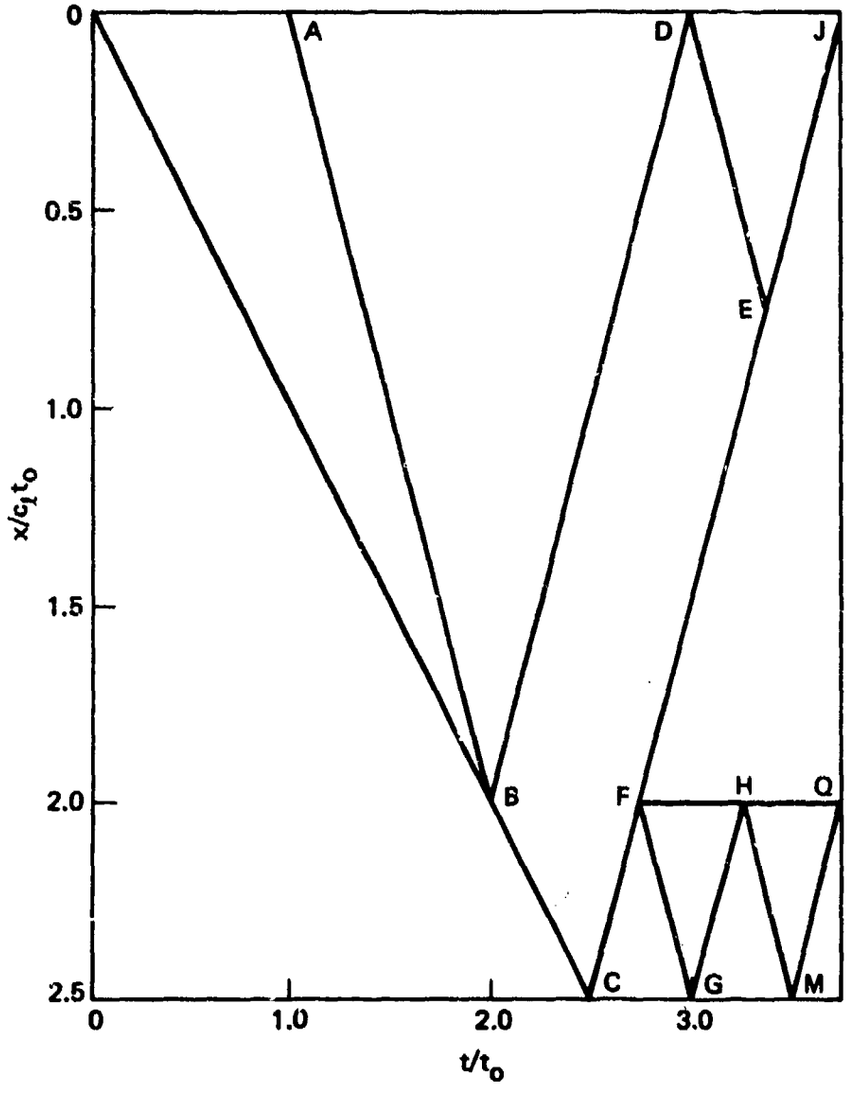

Figure 9. The characteristic plane, redrawn for reference from Figure 8.

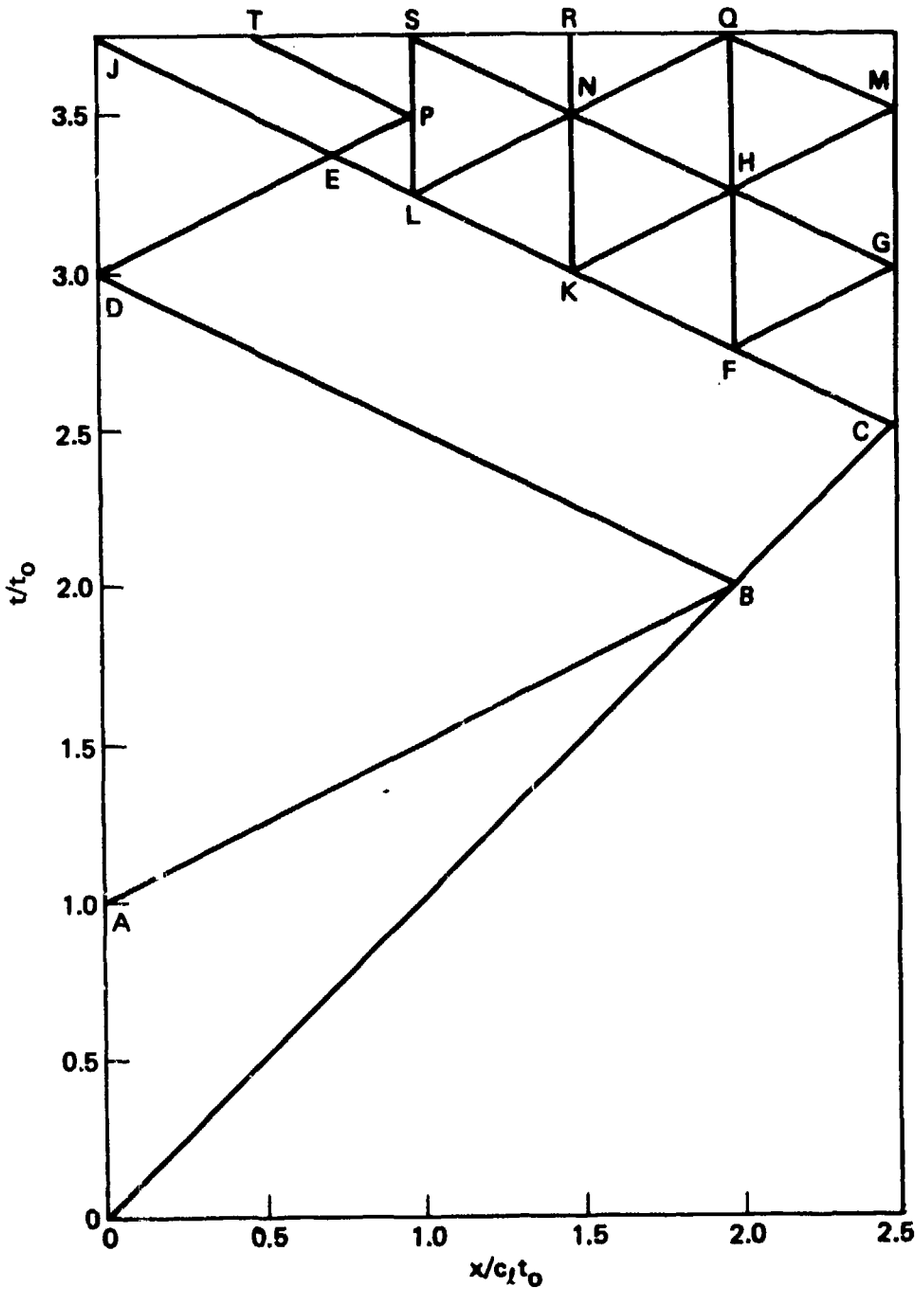

Figure 10. The characteristic plane for cracking by the finite impulse criterion.

A third and final crack will similarly appear at $x = c_\ell t_o$ and $t = 3.25\ t_o$, reflections from its left-hand face not being sufficient to exceed the tensile cutoff at any later times. The stress in the new spalled zones and that to the left of the last crack can be found by the methods already discussed. Profiles are shown in Figure 11 and stress histories in Figure 12. Formulas for the stresses are summarized in Table 1. Note that in Figure 11 there are times and places where the stress at a crack or at the free surface appears not to vanish. This is not in contradiction with the requirement that these surfaces be stress-free; rather, the profiles represent the situation just before a sharp pulse reflects from a free surface.

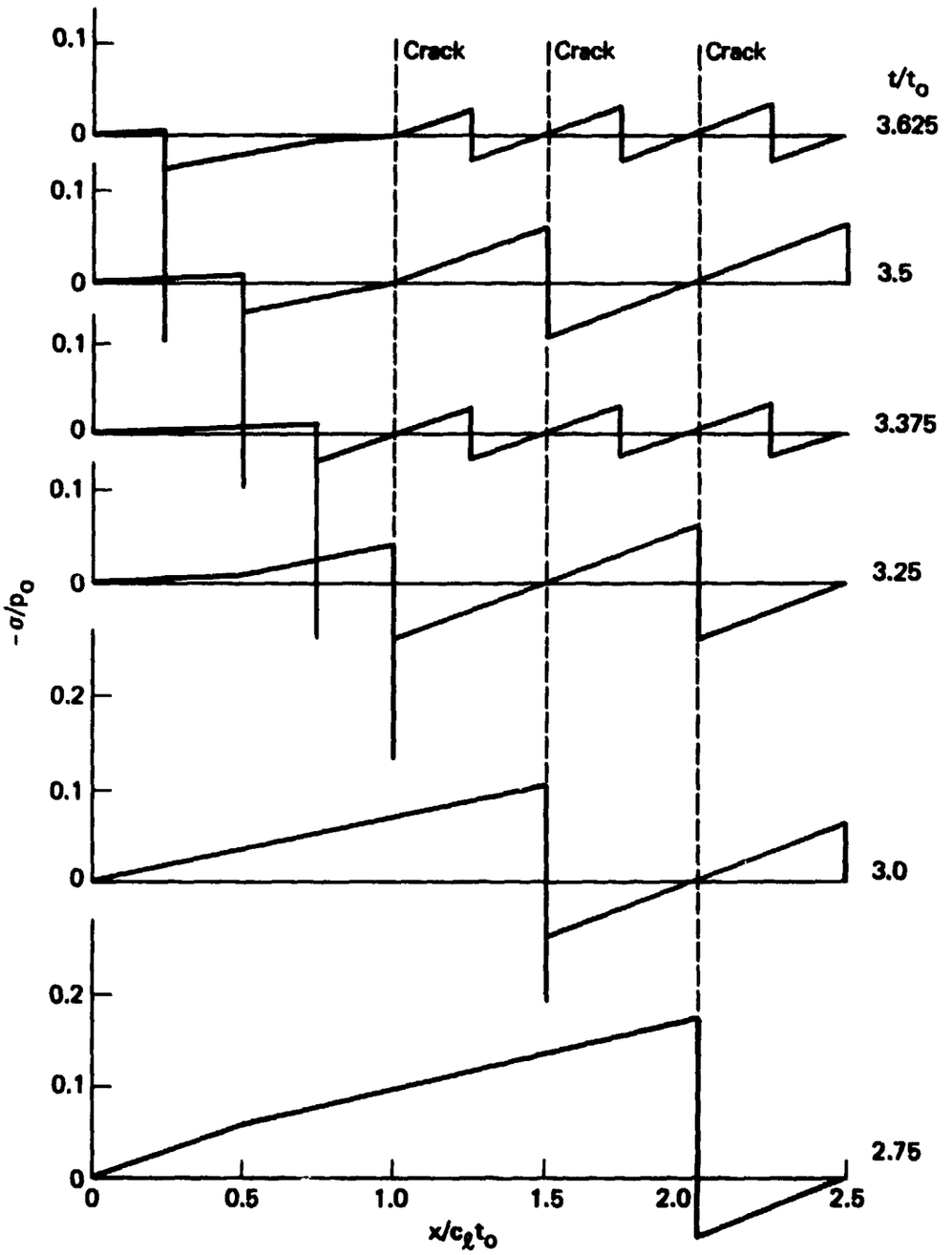

Figure 11. Stress profiles after initial cracking by the finite impulse criterion.

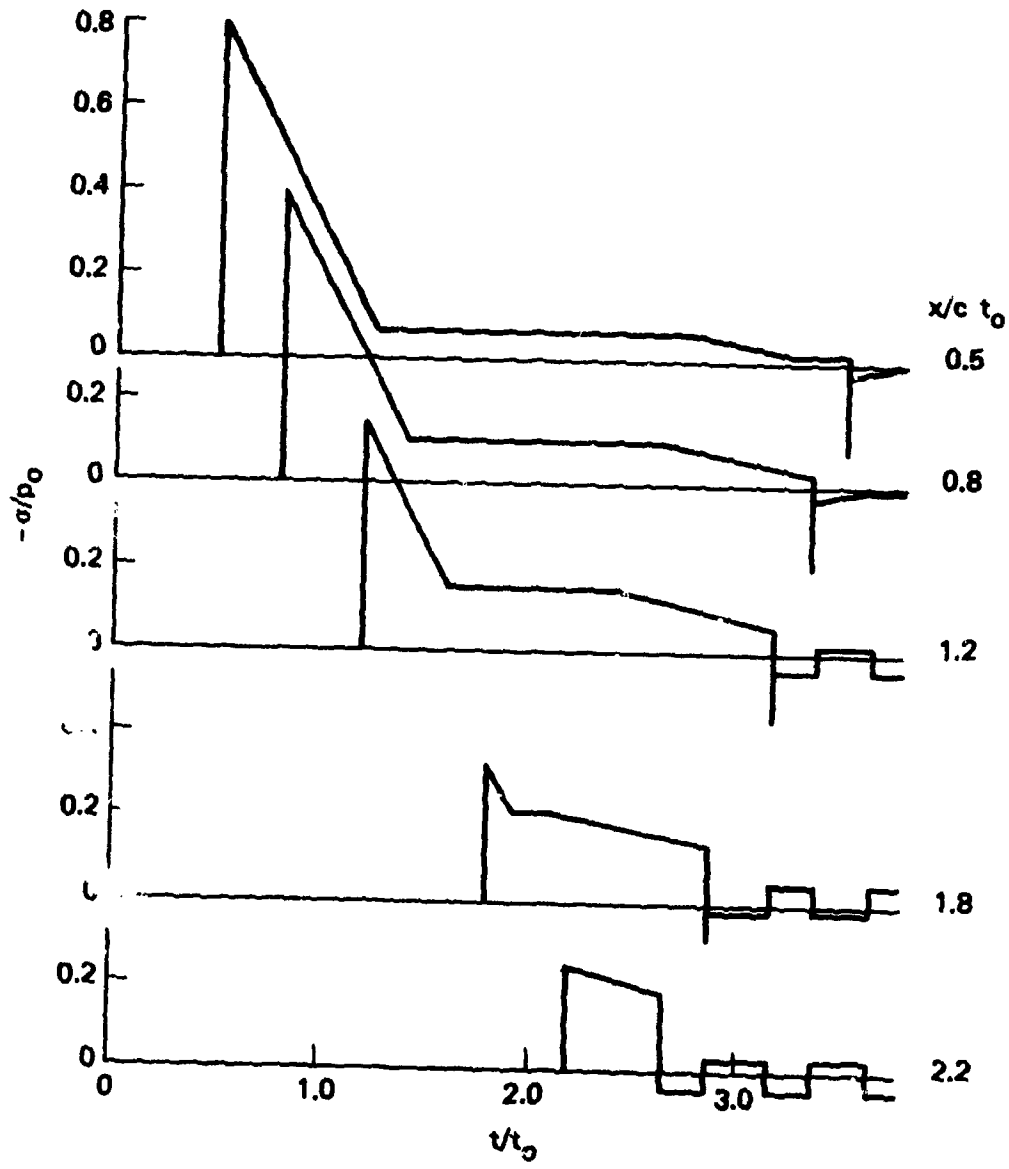

Figure 12. Stress histories in a bilinear solid with a finite tensile impulse cracking criterion.

TABLE 1. FORMULAS FOR STRESS

Region *	$-\sigma(x,t)/p_o$ **
OAB	$1-\tau + (1+\gamma^2)\xi/2$
ABD	$(1-\gamma)^2\xi/2$
BCED	$\frac{1-\gamma}{1+\gamma} + (\frac{1-\gamma}{1+\gamma})^2 [\frac{1+\gamma^2}{2}\xi-\tau]$
DEJ	$(\frac{1-\gamma}{1+\gamma})^2 \frac{(1-\gamma)^2}{2}\xi$
CFG, GHM,...	$-(1-\gamma)^2 (2.5-\xi)/2$
FGH, HMQ,...	$(1-\gamma)^2 (\xi-2.0)/2$
FKH, HNQ,...	$-(1-\gamma)^2 (2.0-\xi)/2$
KHN, NQR,...	$(1-\gamma)^2 (\xi-1.5)/2$
KLN, NRS,...	$-(1-\gamma)^2 (1.5-\xi)/2$
LNS,...	$(1-\gamma)^2 (\xi-1.0)/2$
LEP	$-(1-\gamma)^2 (1.0-\xi)/2$
EPTJ	$-\frac{(1-\gamma)(3-\gamma^2)}{2(1+\gamma)} + (\frac{1-\gamma}{1+\gamma})^2 \left[\frac{1+\gamma^2}{2}\xi+\tau\right]$

* See Figures 5, 9, 10.

** $\tau = t/t_o$, $\xi = x/c_\ell t_o$, $\gamma = c_\ell/c_u$

V. SUMMARY

This report has focused on analytic solutions for stress pulse propagation and reflection and tensile cracking in a slab of one-dimensional bilinear material with a tensile cut-off stress. To aid in the interpretation of events subsequent to the formation of the first crack, guidance has been sought from the analogous problem in an elastic medium. There it was found that after reflection from the free surface, triangular stress pulses of the same height but successively shorter rise times all cause an initial tensile crack at the same location. If a finite tensile impulse is required for cracking, then for sufficiently short rise times (including zero) a narrow tensile spike forms at the reflected wave front ahead of the first crack and propagates back toward the loaded surface without affecting subsequent cracking, even though it exceeds the tension cutoff in magnitude. A broadened tensile pulse that increases linearly from the first crack to the reflected wave front can cause another crack a finite distance from the first when the tensile amplitude builds to a level exceeding the tensile cutoff.

If, on the other hand, only a simple tensile limit need be exceeded but no finite impulse is required for cracking, then the first crack forms as before. The tensile spike tries to form but immediately causes a new crack an infinitesimal distance from the first. A continuously cracked region thus develops ahead of the first crack.

The most important result of the elastic analysis is that in the limit of vanishing rise time, the first crack causes a tensile spike of vanishing width to appear at the reflected wave front. This interpretation has been used to aid in studying the cracking caused by a sharp-fronted triangular pulse in a bilinear material with either a finite

impulse or simple tension cutoff criterion. The propagation and reflection can be treated analytically and in closed form provided the rise time vanishes. Events leading up to the first crack differ from the elastic case in that the pulse changes shape and dissipates energy as it propagates, but share with the elastic case the feature of tensile stress development only after reflection from the free face. The qualitative features of initial crack formation and subsequent crack pattern development are exactly as mentioned above for the elastic case. In particular, a discrete set of cracks appears under the finite impulse criterion, compared with a continuously cracked zone under the simple tensile cutoff criterion.

Because the solution is exact, it may be used to check numerical codes for their ability to model two critical features of constitutive laws for geological materials, viz., hysteresis and tensile cracking behavior. In particular, parametric studies of the effects of zone size and linear and quadratic artificial viscosity may be performed. For the simple tensile cutoff cracking model, the desired numerical solution would contain no spurious cracking in the early stages, and then a sequence of adjacent cracked zones between the first crack and the reflected wave front. Of course, the stress histories of Figure 8 and the profiles of Figures 6 and 7 should be reproduced as well.

Due to the large amount of hysteresis in the assumed material, the pulse amplitude will have decayed substantially before cracking begins. To provide a more definitive check of the tensile cracking feature of a code it may be advisable to start the calculation just prior to initial crack formation. Most codes would ask for initial displacements and velocities as input, and some additional algebra would be required to obtain these from the derived solution.

Velocities at any chosen initial time follow simply from Eq. (6), i.e.,

$$u(x,t) = f'(t-x/c_u) + g'(t+x/c_u) \qquad (22)$$

and the appropriate functions f' and g' can be found by referring to the characteristic plane in Figure 5 and the formulas in the text. Displacements, however, must be obtained by integrating Eq. (22) from the arrival time of the incident wave front at $t = x/c_\ell$ up to the chosen time. Again, Figure 5 will aid in determining which formulas to use for f' and g'.

Future analytical work suggested by the current study is the derivation of closed-form solutions for similar problems in media with more elaborate tensile behavior. Various models for rate-dependent tensile cracking or spall damage accumulation have been put forth and incorporated into numerical codes, but check cases appear to be unavailable. These models have the effect of precluding instantaneous crack formation in favor of a stress-dependent accumulation of damage in the form of void space or distributed cracks. As such, they require a finite tensile impulse for a full crack to develop, although the cracking criterion is not phrased in terms of impulse, nor is the impulse required necessarily a constant. Development of analytical solutions for simple problems in such media would provide valuable check cases for codes incorporating this type of material behavior.

DISTRIBUTION LIST

DEPARTMENT OF DEFENSE

Assistant to the Secretary of Defense
Atomic Energy
ATTN: Executive Assistant

Defense Intelligence Agency
ATTN: DT-1C
ATTN: DB-4C
ATTN: DB-4E4

Defense Nuclear Agency
ATTN: STSP
2 cy ATTN: SPSS
5 cy ATTN: TITL

Defense Technical Information Center
12 cy ATTN. DD

Field Command
Defense Nuclear Agency
ATTN: FCP
ATTN: FCTK

Field Command
Defense Nuclear Agency
Livermore Branch
ATTN: FCPRL

Interservice Nuclear Weapons School
ATTN: TTV

Joint Strat Tgt Planning Staff
ATTN: NRI STINFO, Library
ATTN: JLA

NATO School (SHAPE)
ATTN: U.S. Documents Officer

Under Secretary of Defense for Rsch & Engrg
ATTN: Strategic & Space Sys (OS)

DEPARTMENT OF THE ARMY

Chief of Engineers
Department of the Army
ATTN: DAEN-RDL
ATTN: DAEN-MCE-D

Harry Diamond Laboratories
Department of the Army
ATTN: 00100 Commander/Tech Dir/TSO
ATTN: DELHD-N-P

U.S. Army Ballistic Research Labs
ATTN: DRDAR-BLT, W. Taylor
ATTN: DRDAR-BLT, J. Keefer
ATTN: DRDAR-TSB-S
ATTN: DRDAR-BLV

U.S. Army Concepts Analysis Agency
ATTN: CSSA-ADL

U.S. Army Engineer Center
ATTN: DT-LRC

DEPARTMENT OF THE ARMY (Continued)

U.S. Army Engineer Div, Huntsville
ATTN: HNDED-SR

U.S. Army Engineer Div, Ohio River
ATTN: ORDAS-L

U.S. Army Engr Waterways Exper Station
ATTN: WESSE, L. Ingram
ATTN: WESSD, J. Jackson
ATTN: J. Strange
ATTN: Library
ATTN: WESSA, W. Flathau

U.S. Army Material & Mechanics Rsch Ctr
ATTN: Technical Library

U.S. Army Materiel Dev & Readiness Cmd
ATTN: DRXAM-TL

U.S. Army Missile Command
ATTN: RSIC

U.S. Army Nuclear & Chemical Agency
ATTN: Library

DEPARTMENT OF THE NAVY

Naval Research Laboratory
ATTN: Code 2627

Naval Sea Systems Command
ATTN: SEA-09G53

Naval Surface Weapons Center
ATTN: Code F31

Naval Surface Weapons Center
ATTN: Tech Library & Info Svcs Br

Naval War College
ATTN: Code E-11 (Tech Service)

Naval Weapons Evaluation Facility
ATTN: Code 10

Office of Naval Research
ATTN: Code 474, N. Perrone

Office of the Chief of Naval Operations
ATTN: OP 981
ATTN: OP 03EG

Strategic Systems Project Office
Department of the Navy
ATTN: NSP-43

David Taylor Naval Ship R&D Ctr
ATTN: Code L42-3

Naval Electronic Systems Command
ATTN: PME 117-21

Naval Facilities Engineering Command
ATTN: Code 04B

DEPARTMENT OF THE NAVY (Continued)

Naval Material Command
ATTN: MAT 08T-22

Naval Postgraduate School
ATTN: Code 1424, Library

DEPARTMENT OF THE AIR FORCE

Air Force Institute of Technology
ATTN: Library

Air Force Systems Command
ATTN: DLW

Air Force Weapons Laboratory
Air Force Systems Command
ATTN: NTES-C
ATTN: NTE
ATTN: SUL

Air University Library
Department of the Air Force
ATTN: AUL-LSE

Assistant Chief of Staff
Intelligence
Department of the Air Force
ATTN: INT

Ballistic Missile Office
Air Force Systems Command
ATTN: MMH

Deputy Chief of Staff
Research, Development, & Acq
Department of the Air Force
ATTN: AFRDQI

Deputy Chief of Staff
Logistics & Engineering
Department of the Air Force
ATTN: LEEE

Foreign Technology Division
Air Force Systems Command
ATTN: NIIS, Library

Rome Air Development Center
Air Force Systems Command
ATTN: TSLD

Strategic Air Command
Department of the Air Force
ATTN: NRI STINFO, Library

Vela Seismological Center
ATTN: G. Ullrich

DEPARTMENT OF ENERGY

Department of Energy
Albuquerque Operations Office
ATTN: CTID

Department of Energy
Nevada Operations Office
ATTN: Mail & Records for Technical Library

OTHER GOVERNMENT AGENCIES

Central Intelligence Agency
ATTN: OSWR/NED

Department of the Interior
Bureau of Mines
ATTN: Tech Lib

Department of the Interior
U.S. Geological Survey
ATTN: D. Roddy

Federal Emergency Management Agency
National Sec Ofc Mitigation & Rsch
ATTN: Assistant Associated Dir

DEPARTMENT OF ENERGY CONTRACTORS

Lawrence Livermore National Lab
ATTN: L-10, H. Kruger
ATTN: Technical Info Dept, Library
ATTN: W. Crowley

Los Alamos National Laboratory
ATTN: MS362, Librarian
ATTN: MS 670, J. Hopkins
ATTN: R. Bridwell
ATTN: M. Henderson
ATTN: MS 364
ATTN: G. Spillman

Oak Ridge National Laboratory
ATTN: Central Rsch Library
ATTN: Civil Def Res Proj

Sandia Laboratories
Livermore Laboratory
ATTN: Library & Security Classification Div

Sandia National Lab
ATTN: A. Chabia
ATTN: 3141

DEPARTMENT OF DEFENSE CONTRACTORS

Aerospace Corp
ATTN: Technical Information Services

Agbabian Associates
ATTN: M. Agbabian

Applied Research Associates, Inc
ATTN: N. Higgins
ATTN: J. Bratton

Applied Theory, Inc
ATTN: J. Trulio

Avco Research & Systems Group
ATTN: Library A830

BDM Corp
ATTN: T. Neighbors
ATTN: Corporate Library

Boeing Co
ATTN: Aerospace Library

DEPARTMENT OF DEFENSE CONTRACTORS (Continued)

Boeing Co
ATTN: R. Schmidt

California Institute of Technology
ATTN: T. Ahrens

California Research & Technology, Inc
ATTN: Library
ATTN: K. Kreyenhagen
ATTN: S. Schuster

California Research & Technology, Inc
ATTN: D. Orphal

Calspan Corp
ATTN: Library

University of Denver
ATTN: J. Wisotski

EG&G Wash. Analytical Svcs Ctr, Inc
ATTN: Library

Eric H. Wang
Civil Engineering Rsch Fac
University of New Mexico
ATTN: N. Baum

Gard, Inc
ATTN: G. Neidhardt

Horizons Technology, Inc
ATTN: R. Kruger

IIT Research Institute
ATTN: Documents Library

Institute for Defense Analyses
ATTN: Classified Library

Kaman Avidyne
ATTN: Library

Kaman Sciences Corp
ATTN: Library

Kaman Tempo
ATTN: DASIAC

Lockheed Missiles & Space Co, Inc
ATTN: Technical Information Center
ATTN: T. Geers

Lockheed Missiles & Space Co, Inc
ATTN: TIC-Library

McDonnell Douglas Corp
ATTN: R. Halprin

Merritt CASES, Inc
ATTN: J. Merritt
ATTN: Library

Pacific-Sierra Research Corp
ATTN: H. Brode

Pacifica Technology
ATTN: Tech Library

DEPARTMENT OF DEFENSE CONTRACTORS (Continued)

Patel Enterprises, Inc
ATTN: M. Patel

Physics International Co
ATTN: L. Behrmann
ATTN: E. Moore
ATTN: F. Sauer
ATTN: Technical Library
ATTN: J. Thomsen

R & D Associates
ATTN: J. Carpenter
ATTN: W. Wright
ATTN: J. Lewis
ATTN: Technical Information Center
ATTN: R. Port
ATTN: P. Haas
4 cy ATTN: D. Simons

Science Applications, Inc
ATTN: Technical Library
ATTN: H. Wilson

Science Applications, Inc
ATTN: D. Maxwell
ATTN: D. Bernstein

Science Applications, Inc
ATTN: W. Layson

Southwest Research Institute
ATTN: W. Baker
ATTN: A. Wenzel

SRI International
ATTN: G. Abrahamson

Systems, Science & Software, Inc
ATTN: D. Grine
ATTN: T. Riney
ATTN: T. Cherry
ATTN: R. LaFrenz
ATTN: Library
ATTN: K. Pyatt

Terra Tek, Inc
ATTN: S. Green
ATTN: Library

Tetra Tech, Inc
ATTN: L. Hwang

TRW Defense & Space Sys Group
ATTN: Technical Information Center
ATTN: D. Baer
ATTN: R. Plebuch
ATTN: I. Alber
2 cy ATTN: N. Lipner

TRW Defense & Space Sys Group
ATTN: E. Wong
ATTN: P. Dai

Universal Analytics, Inc
ATTN: E. Field

DEPARTMENT OF DEFENSE CONTRACTORS (Continued)

Weidlinger Assoc, Consulting Engrg
ATTN: J. Wright
ATTN: M. Baron

DEPARTMENT OF DEFENSE CONTRACTORS (Continued)

Weidlinger Assoc, Consulting Engrg
ATTN: J. Isenberg

SUPPLEMENTARY

INFORMATION

AD-A108833

ERRATA SHEET

for

DNA 5738T

STRESS PULSE REFLECTION AND TENSILE CRACKING

IN A ONE-DIMENSIONAL BILINEAR MATERIAL

UNCLASSIFIED

31 December 1980

Please make the following two changes to DNA 5738T:

(1) Add author's name, D. A. Simons, to cover of report.

(2) Change DD Form 1473, Block 20, ABSTRACT, to read:

As a check case for numerical studies of tensile cracking in nonlinear media, closed form solutions have been derived for the following problems. A finite slab of bilinear material is loaded on one face by a sharp-fronted triangular pressure pulse. Cracks are assumed to form in the first case when the stress exceeds a tensile limit, *and in the second case when the stress exceeds a tensile limit for a finite time,* i.e., the tensile impulse is finite. In both cases the stress reaches the tensile limit and a first crack forms shortly after the incident wavefront reflects from the free face of the slab. In the first case a continuously cracked zone develops under the action of a tensile spike caused by the first crack. In the second case, the tensile spike has no effect on cracking, and a sequence of discrete cracks form. Stress histories and stress profiles are plotted for both cases.